Cortical Waves and the Development of Cortical Anatomy.

J. J. Wright [1,2] **and P.D. Bourke** [3]

1. Liggins Institute and Department of Psychological Medicine, University of Auckland, Auckland, New Zealand.
2. Brain Dynamics Centre, University of Sydney, Sydney, Australia.
3. WASP, University of Western Australia, Perth, Western Australia, Australia.

Abstract.

The transmission of waves through the neurons of the cortical mantel, and the development of synapses related to learning, can give rise to the complex structure of neural connections, which emerges during growth of the visual cortex.

Synaptic connections in V1.

In the visual cortex (V1) and cortex generally, the density of synaptic couplings generated by each neuron declines with distance from the soma of the cell of origin, at two scales – that of the local intra-cortical connections (at the V1 macrocolumnar scale), versus the longer intracortical connections (Scholl 1956; Braitenberg and Schuz 1991; Liley and Wright 1994). Thus, visual information can reach each macrocolumn-sized area, from the whole, or a substantial part, of V1. It has been proposed (Wright et al 2006) that via the mediation of waves of brain activity, *local maps of synaptic connections* emerge at the macrocolumnar scale, which form a tiling of V1, each local map being a representation of the visual field – the *global map* - projected to V1 by the visual pathway.

Cortical waves and synchronous fields.

At all scales, the cortex of the brain supports traveling waves of depolarization of the cortical cells, mediated by axonal and dendritic transmission. Theoretically, these waves selectively eliminate of out-of-phase activity during wave interference (Wright 1997; Robinson et al 1998; Wright et al 2000; Chapman et al 2002) explaining the observed occurrence of *synchronous oscillation* (eg, Singer 1994). Because of the decline of synaptic density with distance, the spatial covariance (the magnitude of synchronous oscillation) between any pair of pyramidal neurons in V1 declines with distance Thus, covariance of activity (the average magnitude of synchronous oscillation) in V1 declines with distance at both the global, V1, scale, and the local, macro-columnar, scale. This effect can provide a metric for organization of the local maps from the global map, as follows.

Learning rules and constraints on stable solutions.

At each synapse the co-incidence of pre and post synaptic activity, $r_{Q\varphi}$, over a short epoch, t, is given by

$$r_{Q\varphi}(t) \propto \sum\nolimits_t Q_e(t) \times \varphi_e(t) \qquad (1)$$

where $Q_e(t) \in \{0,1\}$ is the post-synaptic firing rate, and $\varphi_e(t) \in \{0,1\}$ is the pre-synaptic firing rate. A Hebbian multiplication factor, H_s, operating on the gain of synapses at steady states of pre- and post-synaptic firing, in simplest form, is

$$H_s = H_{\max} \exp[-\lambda / r_{Q\varphi}] \qquad (2)$$

where λ is a suitable constant. With changes in $r_{Q\varphi}$, H_s can increase or decline over time. Fields of synchronous oscillation organize the values of $r_{Q\varphi}$ through the cortical field.

Synapses can approach a stable state only by approaching either one of two extremes – with $r_{Q\varphi}$ approaching a maximum (*saturated state)* or a minimum (*sensitive state)* respectively. (These states can correspond to different physiological forms on different time scales.)

Competition occurring for metabolic resources within axons adds a further constraint to stable end-points for synaptic development (Grossberg and Williamson 2001) – viz: the proportion of saturated and sensitive synapses must be uniform along axons.

Overall synaptic stability.

All positions in V1, $\{P_{j,k}\}$, can be given an ordered numbering in the complex plane, $1...,j,...,k,...,2n$, and all positions within a representative macrocolumn located at P_0, $\{p_{j,k}\}$, can be similarly numbered. The total perturbation of synaptic gains in all the synapses from V1 entering the macrocolumn, $\Psi(pP)$, and the total perturbation of synaptic gains within the macrocolumn, $\Psi(pp)$, can be written

$$\Psi(pP)=\sum_{j=1}^{j=n}\sum_{k=1}^{k=n}\sigma_{SAT}(p_jP_k)S_{SAT}(p_jP_k)+\sum_{j=1}^{j=n}\sum_{k=1}^{k=n}\sigma_{SENS}(p_jP_k)S_{SENS}(p_jP_k) \quad (3a)$$

$$\Psi(pp)=\sum_{j=1}^{j=n}\sum_{k=1}^{k=n}\sigma_{SAT}(p_jp_k)S_{SAT}(p_jp_k)+\sum_{j=1}^{j=n}\sum_{k=1}^{k=n}\sigma_{SENS}(p_jp_k)S_{SENS}(p_jp_k) \quad (3b)$$

where $\sigma_{SAT}(p_jP_k,p_jp_k)$ and $\sigma_{SENS}(p_jP_k,p_jp_k)$ are densities of wholly or partially saturated and sensitive synapses respectively, and $S_{SAT}(p_jP_k,p_jp_k)$ and $S_{SENS}(p_jP_k,p_jp_k)$ are the corresponding variations of synaptic gains over a convenient short epoch.
Since densities of synapses decline with distances of cell separation, then as a simple arithmetic property of sums of products, approximation to minimization of $\Psi(pp)$ requires synapses connecting neurons separated by short distances to most closely approach either maximum saturation, or maximum sensitivity. An analogous requirement is imposed on minimization of $\Psi(pP)$, and metabolic uniformity requires that both sensitive and saturated synapses from each axon must remain locally in equal ratio. A stable solution meeting these requirements can be found.

Re-numbering $\{P_{j,k}\}$ as $\{P_{j1,j2,k1,k2}\}$, and $\{p_{j,k}\}$ as $\{p_{j1,j2,k1,k2}\}$, the subscript numbers $1,...,j1,...,j2,...,n,(n+1),...,j2,...,k2,...,2n$ can be ascribed in the global map so that $j1$ and $j2$ are located diametrically opposite and equidistant from P_0, while in the local map $j1$ and $j2$ have positions analogous to superimposed points located on opposite surfaces of a Mobius strip. This generates a *Mobius projection* (the *input map*) from global to local, and a *Mobius ordering* within the local map. That is,

$$\frac{P_{jm}^2}{|P_{jm}|}\rightarrow p_{km} \qquad m\in\{1,2\} \quad (4)$$

and

$$p_{jm}\rightarrow p_{km} \qquad m\in\{1,2\} \quad (5)$$

Evolution of these patterns of synaptic connections is shown in Figures 1 and 2.
In equation (4) the mapping of widely separated points in the global map converge to coincident points on opposite surfaces of the local map's Mobius representation. In equation (5) the density of saturated synaptic connections now decreases as $|j1-k1|$ and $|j2-k2|$, while the density of sensitive couplings decreases as $|j2-k1|$ and $|j1-k2|$.

Anatomically, this requires $j1$ and $j2$ in the local map to represent two distinct groups of neurons. To attain maximum synaptic stability within the local map an intertwined mesh of saturated couplings forms, closed after passing twice around the local map's centre, with sensitive synapses locally linking the two turns of the mesh together. In this fashion both saturated and sensitive synapses decline in density with distance, as required. The input map is of corresponding form, conveying an image of the activity in V1 analogous to projection onto a Mobius strip.

Since the projection of the global map upon the local map conserves relative correlations in

the global map as a function of distance, convergence toward the stable configuration will be facilitated by a modification of the Hebbian rule with a recently demonstrated physiological basis – the *spatio-temporal learning rule* (Tsukada et al 1996; Tsukada and Pan 2005) in which covariance among afferent synapses, as well as pre-postsynaptic neurons, facilitates the strength of synaptic connection.

Figure 1. Initial conditions for local evolution of synaptic strength.
Left. The global field (V1) in polar co-ordinates. Central defect indicates the position of a local area of macro-columnar size. Polar angle is shown by the color spectrum, twice repeated.
Middle. Zones of random termination (shown by color) of lateral axonal projections from global V1 in the local area. Central defect is an arbitrary zero reference.
Right. Transient patterns of synchronous oscillation generated in the local area, mediated by local axonal connections.

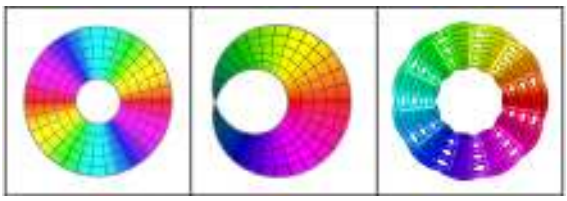

Figure 2. Evolution of synaptic strengths to their maximally stable configuration.
Left. The global field (V1), as represented in Figure 1.
Middle. Saturated synaptic connections input from the global field now form a Mobius projection of the global field, afferent to the local map, forming an input map.
Right. Saturated local synapses within the local map form a mesh of connections closed over $0-4\pi$ radians. The central defect now corresponds to the position within the local map, of the local map within the global map. Sensitive synapses (not shown) link adjacent neurons as bridges between the $0-2\pi$ and $2\pi-4\pi$ limbs of the mesh of saturated connections. Wright et al 2006.

Monosynaptic interactions between adjacent local maps.

Adjacent local maps form in approximately mirror image relation, as shown in Figure 3, because in that configuration homologous points within the local maps have densest saturated and sensitive synaptic connections, thus meeting minimization requirements analogous to those of equations 3(a) and 3(b).

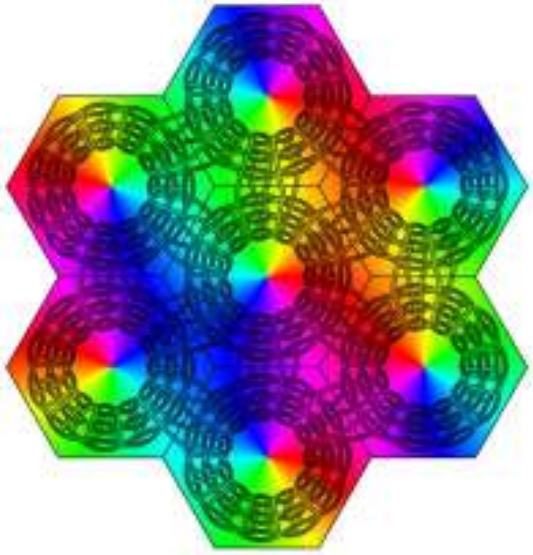

Figure 3. Organization of saturated coupling within and between local maps, and the approximate mirror symmetry of orientation preference in adjacent local maps. Wright et al 2006.

Conformity to experimental data.

These principles can accounts for response preferences of V1 neurons to visual stimuli, orientation preference singularities, linear zones and saddle points, connections between cells of similar orientation preference in adjacent macrocolumns (Bosking et al 1997), ocular dominance columns (Obermayer and Blasdel 1993), occurrence of direction preference fractures always in odd numbers around singularities (Swindale et al 2000) and the dynamic variation of orientation preference with stimulus velocity, stimulus orientation

relative to direction of motion, and stimulus extension, discovered by Basole et al (2003).

References.

Alexander DM, Bourke PD, Sheridan P, Konstandos O, Wright JJ (1998) Emergent symmetry of local and global maps in the primary visual cortex: self-organization of orientation preference. Proceedings Complex Systems 98: 25-31.

Basole A, White LE, Fitzpatrick D (2003) Mapping multiple features of the population response of visual cortex. Nature 423: 986-990.

Bosking WH, Zhang Y, Schofield B, Fitzpatrick D (1997) Orientation selectivity and the arrangement of horizontal connections in tree shrew striate cortex. J. Neuroscience 17(6): 2112-2127.

Braitenberg V, Schuz A (1991) Anatomy of the Cortex: Statistics and Geometry. Springer-Verlag, New York.

Chapman CL, Bourke PD, Wright JJ (2002) Spatial eigenmodes and synchronous oscillation: coincidence detection in simulated cerebral cortex. J. Math. Biol. 45: 57-78.

Grossberg S, Williamson JR (2001) A neural model of how horizontal and interlaminar connections of visual cortex develop into adult circuits that carry out perceptual grouping and learning. Cerebral Cortex 11: 37-58.

Liley DTJ, Wright JJ (1994) Intracortical connectivity of pyramidal and stellate cells: estimates of synaptic densities and coupling symmetry. Network 5; 175-189.

Obermayer K, Blasdel GG (1993) Geometry of orientation and ocular dominance columns in monkey striate cortex. J. Neuroscience 13(10); 4114-4129.

Robinson PA, Rennie CJ, Wright JJ (1998) Synchronous oscillations in the cerebral cortex. Physical Review E 57: 4578-4588.

Scholl DA (1956) The Organization of the Cerebral Cortex. Wiley, New York.

Singer W (1994) Putative functions of temporal correlations in neocortical processing. In: Koch C. and Davis JL (Eds.) Large Scale Neuronal Theories of the Brain. MIT Press, Cambridge Mass., London.

Swindale NV, Shoham D, Grinvald A, Bonhoeffer T, Hubener M. (2000) Visual cortical maps are optimised for uniform coverage. Nature Neuroscience 3(8); 822-826

Tsukada M, Aihara T, Saito H (1996) Hippocampal LTP depends on spatial and temporal correlation of inputs. Neural Networks 9: 1357-1365.

Tsukada M, Pan X (2005) The spatio-temporal learning rule and its efficiency in separating spatiotemporal patterns. Biological Cybernetics 92: 139-146.

Wright JJ (1997) EEG simulation: variation of spectral envelope, pulse synchrony and 40 Hz oscillation. Biological Cybernetics 76: 181-184.

Wright JJ, Bourke PD, Chapman CL (2000) Synchronous oscillation in the cerebral cortex and object coherence: simulation of basic electrophysiological findings. Biological Cybernetics, 83: 341-353.

Wright JJ, Alexander DM, Bourke PD (2006) Contribution of lateral interactions in V1 to organization of response properties. Vision Research 46: 2703-2720.